IDENTIFYING OLIVINE IN LIBYA MONTES AND TYRRHENA TERRA, MARS. M. D. Lane[1], D. Tirsch[2], J. L. Bishop[3], C. Viviano[4], D. Loizeau[5], L. L. Tornabene[6], and R. Jaumann[2,7] [1]Fibernetics LLC, Lititz, PA (lane@fibergyro.com), [2]Institute of Planetary Research, German Aerospace Center (DLR), Berlin, Germany, [3]Carl Sagan Center, SETI Institute, Mountain View, CA, USA, [4]Dept. of Earth Sciences, Centre for Planetary Science and Exploration, University of Western Ontario, London, Canada, [5]Johns Hopkins University Applied Physics Lab (JHUAPL), Laurel, Maryland, USA, [6]University of Lyon, Lyon, France, [7]Institute of Geological Sciences, Freie Universität Berlin, Berlin, Germany.

Introduction: A variety of aqueous alteration materials as well as unaltered mafic rocks have been identified by investigations across the region between Isidis and Hellas [e.g., 1, 2, 3, 4, 5, 6]. Exposed views of ancient crustal rocks, lava flows from Syrtis Major, alteration from the large Isidis and Hellas impacts, and multiple stream beds and deltas make this region unique on Mars [e.g., 7, 8, 9, 10]. Previous studies of morphologic and spectroscopic features using coordinated CRISM-HRSC and CRISM-HiRISE-CTX imagery observed distinct stratigraphic units containing phyllosilicates, carbonate, olivine and pyroxene in isolated regions [e.g., 11, 12]. Tirsch et al. [13] extended that work across a broader area of Libya Montes and south across Tyrrhena Terra in order to 1) characterize the types and occurrences of phyllosilicates, opal, zeolites, and carbonates; 2) assess relationships between these aqueous outcrops and surface features such as craters, aqueous channels, and deltas; 3) investigate whether the surface rocks were altered by the Syrtis flows or Isidis impact; 4) determine relationships between smaller craters (e.g., Dulovo, Hashir, Bradbury, Lipany, Auki, and Lopez) and the surface rocks; 5) evaluate the surface mineralogy across the study region in relation to thermal inertia and elemental abundances; and 6) determine the effects of impact alteration in formation or transformation of the mineralogy.

In order to build on previous investigations by Tirsch et al. [13], this work begins to address the olivine present in the region of study using thermal (mid-) infrared data from the Mars Global Surveyor Thermal Emission Spectrometer (hereafter TES) and Mars Odyssey Thermal Emission Imaging System (hereafter THEMIS). Our team is investigating the mineralogy in the region using a broad array of spectral data sets from the visible (VIS) through the mid-infrared (MIR).

Olivine Spectral Index: Olivine spectral indices were developed for spectra of 13 synthetic olivine pressed powders that ranged in composition from the Mg end member forsterite (Fo100) to the Fe end member fayalite (Fo0). Presentation of the entire range of Mg-Fe solid solution spectra can be found in [14]. By developing a spectral index that maps a feature that shifts with composition, Lane and Christensen [15] have previously applied the olivine indices to TES data using Java Mission-planning and Analysis for Remote Sensing (JMARS) software [16]. In [15], application of the olivine index to orbital data the Gale Crater dunes, allowed the olivine composition in the Bagnold Dunes to be identified as Fo55 (+/-5). This composition was verified on the ground by the *Curiosity* rover using CheMin data that identified the olivine as Fo56 (+/-3) [17].

Knowing the methodology for determining olivine composition works, the olivine indices were applied to TES data of our study site. In order to apply the developed spectral indices to interpreting the TES data from Mars, the laboratory spectra (at 2 cm^{-1} spectral resolution) were degraded to the ~10 cm^{-1} spectral resolution to identify correct TES bands for the index formulae. Because of the coarseness of the TES spectral resolution, some Fo#s are represented by an equation identical to a neighboring Fo#. This was the case for Fo50 and Fo55, as well as Fo70 and Fo75, indicating a minimum error in compositional determination of +/-5 Fo#.

Figure 1 shows the TES olivine index mapping of Fo50/55 in the top panel and Fo65 in the middle panel. Where more olivine of that composition is mapped, the pixels appear as warmer colors (toward red). Lesser (or no) olivine maps as cooler colors (toward blue). In this region, the index is showing mid-range amounts of olivine as more-or-less intense green.

Compositional Results: The TES data (from the index maps alone in Fig. 1) suggest the Martian basaltic Tyrrhena Terra region is dominated by mid-range composition olivine (~Fo50/55 to Fo65). Although the Fo65 map shows olivine in more isolated sites, this map jibes more closely to the bottom map in Fig. 1 that is from [13]. The bottom map shows the visible-range Compact Reconnaissance Imaging Spectrometer (CRISM) data [18] where olivine is mapped in green (Fe/Mg-bearing phyllosilicates are mapped in red; low-Ca pyroxene is mapped in blue).

The TES olivine index maps are not designed to identify locations of phyllosilicates or pyroxenes; however, future work will be focused on mapping those minerals as well as the olivine.

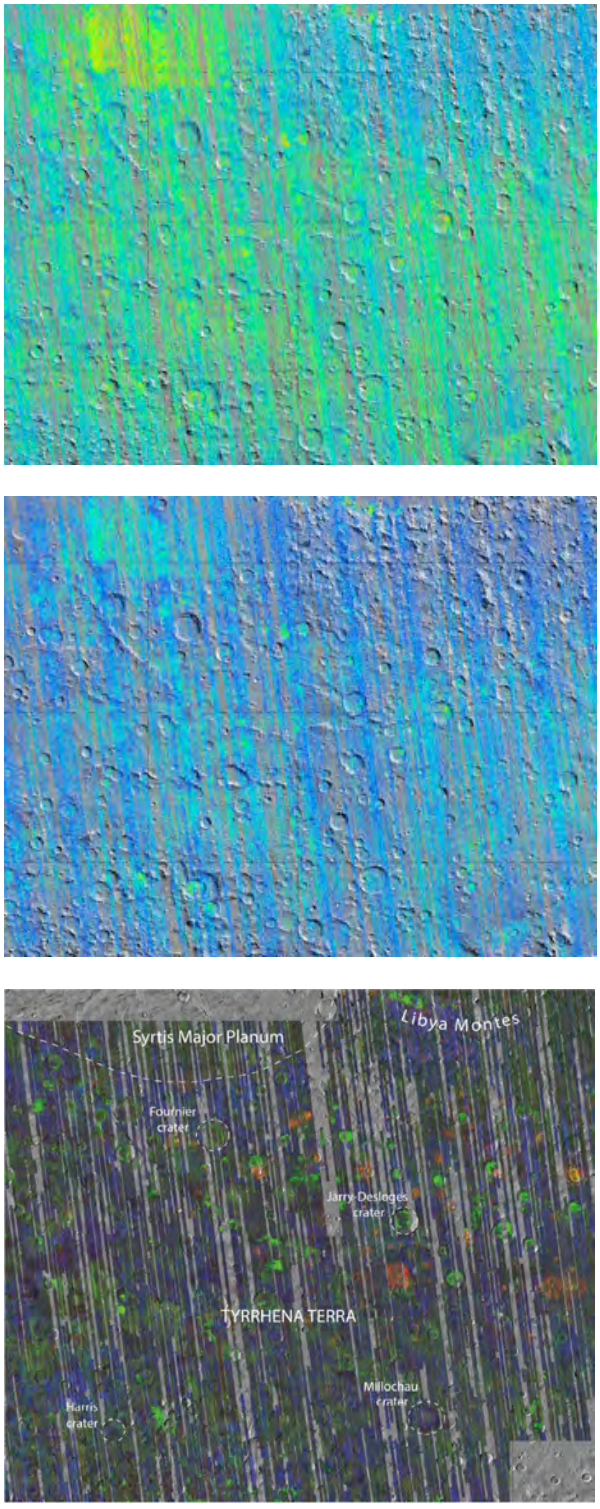

Figure 1. Spectral index maps of olivine for Fo50/55 and Fo65 (top and middle, respectively) as determined using TES data. Red-Green-Blue (RGB) composite of CRISM data showing olivine mapped to green. (See text for further discussion of colors.)

Future Work: This region will be studied in a lot more detail using multiple data sets acquired at Mars, especially from the Mars Reconnaissance Orbiter, Mars Express, Mars Global Surveyor and Mars Odyssey spacecraft. We will be coordinating our multi-instrument and multi-wavelength spectral analyses to maximize the understanding of the geology of this region.

References: [1] Craddock R.A. (1994), *LPSC XXV,* Abstract #291. [2] Ivanov M.A. & Head J.W. (2003) *JGR, 108,* E6. [3] Rogers A.D. & Christensen P.R. (2007) *JGR, 112,* E01003. [4] Tornabene L.L. et al. (2008) *JGR, 113,* E10001. [5] Loizeau D. et al. (2012) *Icarus, 219,* 476-497. [6] Rogers A.D. & Hamilton V.E. (2015) *JGR, 120*, 62-91. [7] Crumpler L.S. & Tanaka K.L. (2003) *JGR, 108,* 12. [8] Jaumann R., et al. (2010) *EPSL, 294,* 272-290. [9] Erkeling G., et al. (2012) *Icarus, 219*, 393-413. [10] Ivanov, M.A., et al. (2012) *Icarus, 218,* 24-46. [11] Bishop J.L., et al. (2013) *JGR, 118,* 487–513. [12] Tirsch, D., et al. (2018) *Icarus, 314,* 12-34. [13] Tirsch et al. (2019) 50th LPSC, Abstract #1532. [14] Lane et al. (2011) *JGR 116,* E08010. [15] Lane, M.D. & Christensen P.R. (2013) *GRL, 40,* 1-5. [16] Christensen P.R. et al. (2009) *EOS Trans. AGU., 90*(52), Fall Meet. Suppl., Abstract #IN22A-06. [17] Achilles C.N. et al. (2017) *JGR 122,* doi:10.1002/2017JE005262. [18] Murchie S.L., et al. (2009) *JGR, 114,* E00D06.